# Supporting Online Material for

## Cortical Plasticity Induced by Inhibitory Neuron Transplantation

Derek G. Southwell, Robert C. Froemke, Arturo Alvarez-Buylla,*
Michael P. Stryker,* Sunil P. Gandhi*

*To whom correspondence should be addressed.
E-mail: abuylla@stemcell.ucsf.edu (A.A.B.); stryker@phy.ucsf.edu (M.P.S.);
sunil@phy.ucsf.edu (S.P.G.)

Published 26 February 2010, *Science* **327**, 1145 (2010)
DOI: 10.1126/science.1183962

**This PDF file includes:**

**Supporting online material**

**Author contributions** D.G.S., R.C.F., A.A.-B., M.P.S. and S.P.G. designed experiments. D.G.S. performed transplantation and histology. R.C.F. made electrophysiological recordings. S.P.G. performed studies of ocular dominance plasticity. D.G.S., R.C.F. and S.P.G. analyzed the histological, electrophysiological and optical imaging data, respectively. D.G.S. and S.P.G. wrote the manuscript. R.C.F., A.A.-B and M.P.S. edited the manuscript.

**Materials and Methods**

**Animals** All protocols and procedures followed the guidelines of the Laboratory Animal Resource Center at the University of California, San Francisco. Embryonic donor tissue was produced by crossing CD-1 wild-type mice to homozygous green fluorescent protein-expressing (GFP) mice (*S1*) or homozygous Discosoma red fluorescent protein-expressing (DsRed) mice (*S2*). GAD67-GFP(del-Neo) host mice (*S3*) were produced by crossing heterozygous GAD67-GFP mice to wild-type C57Bl/6 mice. GAD67-GFP offspring were genotyped under an epifluorescence dissection microscope. Wild-type host mice were obtained from Jackson Laboratories. Wild-type C57Bl/6 and CD-1 breeder mice were obtained from Charles River Laboratories. All experimental and control animals experienced identical housing conditions throughout postnatal life and the period of monocular visual deprivation.

**Tissue dissection** The ventricular and subventricular layers of the medial ganglionic eminence (MGE) or lateral ganglionic eminence (LGE) were dissected from embryonic day 13.5 (E13.5) to E14.5 GFP or DsRed donor embryos. Embryonic day 0.5 was defined as the time when the sperm plug was detected. Embryonic MGE explants were dissected in Liebovitz L-15 medium containing DNaseI (100 μg/ml), and mechanically dissociated into a single cell suspension by repeated pipetting. The dissociated cells were then concentrated by centrifugation (3 min, 3000 r/min).

**Cell transplantation** Concentrated cell suspensions (~$10^3$ cells/nl) were loaded into beveled glass micropipettes (~50 μm tip diameter; Wiretrol 5 μl, Drummond Scientific Company).

Micropipettes were positioned at an angle of 15 degrees from vertical in a stereotactic injection apparatus. All host mice were anesthetized by hypothermia and positioned in a clay head mold that stabilized the skull (*S4*). Approximately $10^5$ cells (100 nl) were transcranially injected into each of two sites (2 x $10^5$ cells, total) in the caudal portion of the left cerebral cortex, as depicted in Figures 1 and S1. The X-Y coordinates of the injection sites were estimated by surface anatomy, and placed outside the binocular region of primary visual cortex. The Z coordinates (depth) of the injection sites were 0.7 mm below the skin surface. For dead-cell experimental controls, equal volumes of freeze-thawed, dead MGE cells were injected. Immediately after the injections were completed, animals were placed on a warm surface until they became active. The host mice were then returned to their mothers until they reached weaning age (P20).

**Monocular deprivation** Monocular visual deprivation was produced by suturing the right eyelid shut, contralateral to the transplanted- or control-treated left occipital cortex, according to procedures described previously (*S5*). Animals were checked daily to confirm that the eyelids remained shut for 4 days. Mice whose eyelids opened prematurely, or whose corneas showed signs of damage, were removed from the study. The monocular deprivation procedure was performed on hosts and control animals 17, 25-27, 33-35 and 43-46 days after transplantation (Figure 1B).

**Surgical procedures for repeated transcranial optical imaging** The surgical preparation for repeated optical imaging of intrinsic signals has been described in detail elsewhere (*S6*). Briefly, animals were anesthetized with 2-3% Isoflurane supplemented with a single intraperitoneal injection of chlorprothixene (1 mg/kg) and placed in a stereotaxic frame. Subcutaneous injections of atropine (0.3 mg/kg) and caprofen (5 mg/kg) were delivered to reduce secretions and to provide post-operative analgesia, respectively. Animals were maintained at a body temperature of 37.5°C using a heating pad under feedback control from a rectal thermoprobe. The skull over the left occipital cortex was exposed and covered with agarose and a coverslip. The eyes were protected with a thin coat of silicon oil. Optical imaging was performed under stable anesthesia with 0.7-0.9% isoflurane. The concentration of isoflurane was continually monitored using an Ohmeda 5250 RGM (Datex-Ohmeda). At the conclusion of the first recording session, the monocular deprivation procedure was performed. Animals were returned

to their cages once they recovered normal awake behavior, no more than 2-3 hours after isoflurane was discontinued. Four days later, the sutured eyelid was opened and the skull was exposed at the same location for the subsequent recording session. For some experiments, recordings were performed using a single, acute transcranial preparation. At the end of the final imaging session, the boundaries of binocular primary visual cortex were marked with penetrations of fine tungsten wire coated in DiI (Invitrogen) according to the maps produced by optical imaging.

**Optical imaging of the eye-specific responses to visual stimulation** Optical images of visual cortex were acquired directly through the skull as described earlier (*S7, S8, S9*). Briefly, a Dalsa 1M30 CCD Camera (Dalsa), equipped with a 135 X 50 mm tandem lens (Nikon), gathered images of 610 nm light reflected by the visual cortex at 7.5 Hz and 512 x 512 resolution. The focal plane of the optics was positioned 550-650 μm beneath the blood vessels on the surface of the brain. During the recording sessions, animals viewed a contrast-modulated stochastic noise movie (*S10, S11*). The temporal spectrum of the movie was flat with a sharp low-pass cutoff of 4 Hz. A smooth spatial low-pass cutoff was applied at 0.05 cyc/deg. The noise movie was cropped so that it only appeared within the limits of the mouse binocular visual field (- 5 to +15 deg azimuth). Finally the noise movie was multiplied by a sinusoidally varying contrast (frequency = 0.1 Hz). The noise movie was presented on a high refresh rate monitor placed 25 cm in front of the animal. The movie was presented alternately to each eye in 5 min durations. Cumulatively, responses were recorded for 10-20 min for each eye.

**Immunostaining** After optical imaging was completed and the binocular visual cortex was marked by DiI injection, animals were transcardially perfused with 4% paraformaldehyde. The brains were removed, postfixed overnight in 4% paraformaldehyde, and cryoprotected in 25% sucrose. Coronal brain sections (50 μm) were cut using a frozen sliding microtome. Floating sections were immunostained with the following primary antibodies: chicken anti-GFP (1:500; Aves Labs), rabbit anti-DsRed (1:500; Clontech), rabbit anti-calbindin (1:3000; SWANT), rabbit anti-calretinin (1:750; SWANT), rabbit anti-neuropeptide Y (1:1250; Immunostar), mouse anti-parvalbumin (1:4000; Chemicon), and rabbit anti-somatostatin (1:300; Bachem). The following secondary antibodies were used: Alexa Fluor 488 goat anti-chicken, Alexa Fluor 488 goat anti-mouse, Alexa Fluor 594 donkey anti-rabbit, Alexa Fluor 594 donkey anti-mouse (1:500;

Molecular Probes). Tissue blocking and antibody incubations were made using a solution of 2% bovine serum albumin, 8% normal goat serum, and 0.5% Triton X-100 in PBS. Sections were blocked for 1 hour at room temperature, incubated in primary antibody solutions overnight at 4°C, and incubated in secondary antibody solutions for 1.5 hours at room temperature. After the primary and secondary antibody incubations were finished, sections were washed four times in PBS. After the second series of washes, the sections were mounted on glass slides and coverslipped.

**Cell quantification and molecular characterization** Cell density and spatial distribution measurements were made within the boundaries of binocular primary visual cortex, as defined by the DiI tracks. First, using a 20x objective, transplanted cell profile counts were made in all cortical layers of three 50 μm coronal sections: the rostral and caudal sections included the rostral and caudal limits of the DiI-labeled cortex, respectively, while the middle section was equidistant from the rostral and caudal sections (approximately 400 μm separated each section). To ensure that comparisons of cell profile counts were not biased by cell-size differences between the various groups, we measured the maximum widths of transplanted cell profiles (17 DAT = 10.6±0.2 μm, n = 79 cells; 25-27 DAT = 10.6±0.2 μm, n = 108; 33-35 DAT to P9-11 hosts = 11.6±0.2 μm, n = 183; 43-46 DAT = 12.2±0.2 μm, n = 145). Cell density measurements were then obtained by dividing the total transplanted cell profile count by the total area of the DiI-labeled cortex in the three sections (17 DAT, n = 4 animals; 25-27 DAT, n = 6; 33-35 DAT to P0-2 hosts, n = 5; 33-35 DAT to P9-11 hosts, n = 12; 43-46 DAT, n = 5). For each host, the rostral-caudal spatial distributions were calculated by dividing the transplanted cell profile counts obtained from each of the three sections by the total transplanted cell profile count from all three sections. To measure the distribution of transplanted cells across the depth of the cortex, the sampled area of visual cortex was divided into halves along its depth (from the pia to the white matter). The distribution of cells in the upper half of cortex was then calculated by dividing the profile count obtained from the upper half of the cortex in the three sections by the total profile count from all three sections. The morphological phenotypes of all counted cells were examined (3562 cells total, n = 33 animals).

The molecular phenotypes of transplanted GFP-labeled cells were measured in the group studied at 33-35 DAT. For each marker (calbindin, calretinin, neuropeptide Y, parvalbumin, somatostatin), three or four sections (at intervals of 600 μm between sections) were used for quantification. Two of the sampled sections included the binocular visual cortex, as indicated by the DiI injections, while the remainder of the sections were immediately rostral or caudal to binocular visual cortex (calbindin, 171 of 766 cells; calretinin, 142 of 800; neuropeptide Y, 88 of 909; parvalbumin, 198 of 709; somatostatin, 461 of 932; n=6 animals). The percentage of transplanted cells that expressed parvalbumin was measured in all experimental groups (17 DAT, 84 of 623 cells, n = 4 animals; 25-27 DAT, 102 of 506, n=5; 33-35 DAT to P9-11 hosts, 326 of 1278, n = 12; 43-46 DAT, 192 of 580, n=5)

**Histological imaging** Histological images shown in Figure 2 were produced using a confocal microscope (Leica SP5). Figures 2A and 2B represent flattened Z-series of confocal slices (12 slices, 1.5 μm per slice). Figure 2C depicts a single confocal slice of 1 μm thickness. Image shown in Figure S3 represents a flattened Z-series of confocal slices (18 slices, 2.5 μm per slice). Images were adjusted for brightness and contrast with Adobe Photoshop CS3 (Adobe Systems Inc.).

**Analysis of optical imaging data** A map of responses in binocular visual cortex was extracted from the optical imaging data using Fourier analysis. For each pixel, the Fourier component corresponding to the frequency of contrast modulation in the visual stimulus (0.1 Hz) was computed as described earlier (*S7*). The response map generated by this calculation was then smoothed with a 5 x 5 pixel uniform filter and cropped to isolate the region corresponding to the visual cortex. The maximum amplitude in the smoothed, cropped region was taken to represent the overall strength of the response. The ocular dominance index (ODI) was then computed as (**C**-**I**)/(**C**+**I**), where **C** represents the response strength to contralateral eye stimulation and **I** represents the response strength to ipsilateral eye stimulation. Calculations of ODI using the maximum of the smoothed amplitude response maps agree closely with an alternative method for calculating ODI based on a pixel-wise comparison of the ipsi- and contralateral maps (*11*). An ocular dominance shift was quantified for each animal as the difference between the ODI value measured before and the ODI value measured after monocular deprivation. Fourier analysis was

performed using custom written software (*9*) and map amplitude calculations in custom-written Matlab routines (Mathworks).

**Statistical analysis of optical imaging data** A Mann-Whitney two-tailed test was used to assess the significance of differences in ODI values measured after monocular deprivation. Kruskal-Wallis analysis of variance was used to determine significance of differences in ocular dominance shift across experimental groups. All statistical analyses were performed using Prism 4.0 (Graphpad).

**Visual cortical slice preparation** Transplantation was performed at P0-2 or P9-11 and slices of host brains were prepared at P43±4 (mean±s.d.) for transplanted cell recordings and at P45±6 for host cell recordings. Transplanted cell recordings were made 36±3 DAT and host cell recordings were made 38±4 DAT. Both sets of recordings spanned the period when transplant-induced plasticity was strongest (33-35 DAT plus 4 days of monocular deprivation; see Figure 1). Animals were deeply anesthetized with urethane, decapitated, and the brains were quickly placed into ice-cold dissection buffer containing (in mM): 252 sucrose, 3 KCl, 2 MgSO4, 1.25 NaH2PO4, 26 NaHCO3, and 10 dextrose, bubbled with 95% O2 / 5% CO2 (pH 7.4). Coronal slices (400 μm thickness) of visual cortex were prepared with a vibratome (Leica) and transferred to a holding chamber containing oxygenated artificial cerebrospinal fluid (ACSF; (in mM) 126 NaCl, 3 KCl, 2 MgSO4, 1.25 NaH2PO4, 2 CaCl2, 26 NaCHO3, and 10 dextrose), and kept at 33-35°C for >1 hr before use.

**Electrophysiology** Whole-cell recordings were made in current-clamp mode with a Multiclamp 700B amplifier (Molecular Devices) using IR-DIC video microscopy. Patch pipettes (4-9 MW) were filled with intracellular solution (in mM: 130 K-gluconate, 10 HEPES, 0.2 EGTA, 4 KCl, 2 NaCl, 14 phosphocreatine, 4 Mg-ATP, and 0.3 Na-GTP). Data were filtered at 10 kHz, digitized at 20 kHz, and analyzed with Clampfit 10 (Axon). Control cells were recorded in slices made from P45±6 animals (mean±s.d.), and transplanted cell recordings were recorded in slices made from P43±4 animals ($p>0.2$, two-tailed Student's t-test).

*Percentage of Fast Spiking Cells* Inhibitory neurons were selected for recording primarily by fluorescence, but morphological and electrophysiological criteria were also used in many cases. In a subset of recordings, spiking properties were more completely characterized with prolonged current injections (usually 600 ms, ± 0-400 pA) to classify the inhibitory cells into fast spiking (FS) and non-fast spiking types (Figure S9). Ten of twenty-nine (34.5%) transplanted inhibitory neurons were FS cells, which was similar to the proportion of host FS inhibitory neurons (11/25 or 44.0%; $p>0.5$, Fisher's two-tailed exact test).

*Resting Membrane Potential, Input Resistance and Spike Threshold* Series and input resistances were monitored with hyperpolarizing current pulses (–40 pA, 600 ms), and were similar across cell types (series resistance of host pyramidal neurons, 15.6±6.7 MΩ (mean±s.d.); host inhibitory neurons, 13.5±6.4 MΩ; transplanted inhibitory neurons, 14.0±7.1 MΩ; $p>0.8$; input resistance of host pyramidal neurons, 143.0±90.3 MΩ; host inhibitory neurons, 142.3±80.4 MΩ; transplanted inhibitory neurons, 150.6±60.3 MΩ; $p>0.8$). Resting membrane potential was set with current injection to be -70 mV for recording EPSPs in inhibitory neurons, and -45 mV for recording IPSPs in pyramidal cells. Resting membrane potentials and spike thresholds were not significantly different between host and transplanted inhibitory neurons (membrane potential of host pyramidal neurons, –72.6±13.0 mV; host inhibitory neurons, –81.1±11.3 mV; transplanted inhibitory neurons, –72.1±9.4 mV; $p>0.1$ compared to host inhibitory; spike threshold of host pyramidal neurons, –47.4 ±10.1 mV; host inhibitory neurons, –54.8±5.9 mV; transplanted inhibitory neurons, –51.7 ±4.7 mV; $p>0.1$). Postsynaptic potentials were evoked by stimulating the putative presynaptic cell with pairs of depolarizing current steps separated by 50 ms.

*Percentage of Dual Whole-Cell Recordings* Approximately one-third of potential connections were assessed with dual whole-cell recordings. By type, the percentages of dual whole-cell recordings were $E_{host}$-to-$I_{trans}$, 11/35 or 31.4%; $E_{host}$-to-$I_{host}$, 17/47 or 36.2%; $I_{trans}$-to-$E_{host}$, 12/24 or 50.0%; $I_{host}$-to-$E_{host}$, 17/43 or 39.5%. The remaining connections were assessed with loose-patch stimulation of the putative presynaptic neurons.

*Intensity of Loose-Patch Stimulation* The intensity of loose-patch current-clamp stimulation was similar for each of the connections tested ($E_{host}$-to-$I_{trans}$, 2.4±1.0 nA (mean±s.d.); $E_{host}$-to-

$I_{host}$,1.8±0.4 nA; $I_{trans}$-to-$E_{host}$, 1.8±1.1 nA; $I_{host}$-to-$E_{host}$, 2.0±0.7 nA). Durations of stimulation were 1-5 ms in all recordings. Cells were considered connected if events were larger than twice the standard deviation of the baseline noise. Connection strength was measured as the EPSP or IPSP peak (assessed in a 1 ms window around the maximum absolute value). Statistical analysis was performed with the two-tailed version of Fisher's exact test.

# Figure S1

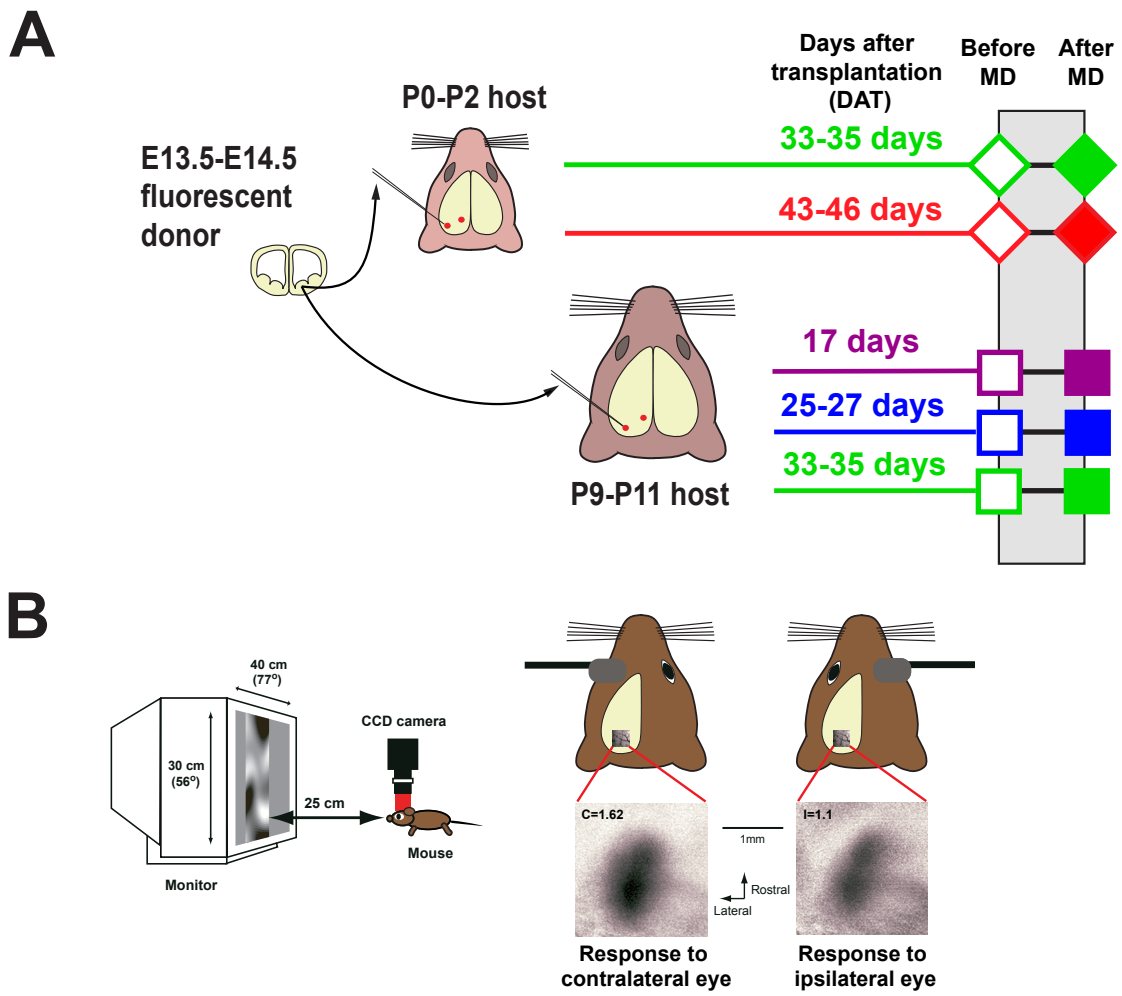


**Figure S1. Inhibitory neuron precursor transplantation and optical measurements of visual responses. (A)** Inhibitory neuron precursors were transplanted from embryonic day 13.5-14.5 (E13.5-14.5) DsRed- or GFP-labeled donors to postnatal host mice. Primary cell suspensions were injected through a glass capillary needle into two sites (red circles) that flanked primary visual cortex. Embryonic cells were transplanted to postnatal day 0-2 (P0-2; diamonds) and P9-11 (squares) GAD67-GFP or wild-type mice, and then left to develop in the host brain for 17, 25-27, 33-35, or 43-46 days. Host animals then underwent 4 days of monocular visual deprivation (MD) contralateral to the transplanted hemisphere before ocular dominance plasticity was assessed by optical imaging of intrinsic signals. Open symbols represent visual response measurements made immediately before MD, while solid symbols represent measurements made immediately after MD. **(B)** Visual responses were measured using optical imaging of intrinsic signals. A band-limited, contrast-modulated noise stimulus, designed to drive responses from nearly all neurons in primary visual cortex, was displayed within the binocular visual field (-5 to 15 deg). Reflected 610 nm light was imaged through the skull while the stimulus was viewed alternately through the contra- and ipsilateral eye every 5 minutes. Responses were extracted using Fourier analysis. The response amplitude for each eye was taken as the peak value of the smoothed Fourier map. An ocular dominance index (ODI) for each recording session was computed from the two responses.

# Figure S2

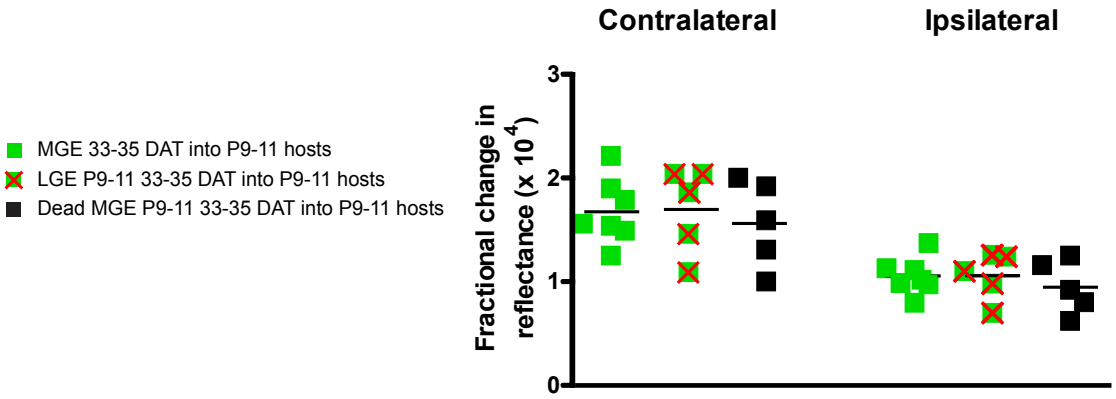


**Figure S2. The magnitudes of visual responses are similar in animals that receive live MGE cell transplants, live LGE cell transplants, and dead MGE cell transplants.** Responses to visual stimulation through the contralateral and ipsilateral eyes are shown for various experimental groups studied at P42-46, 15-20 days after the critical period. All animals received transplants at P9-11. All measurements were made before monocular visual deprivation, 33-35 days after transplantation.

# Figure S3

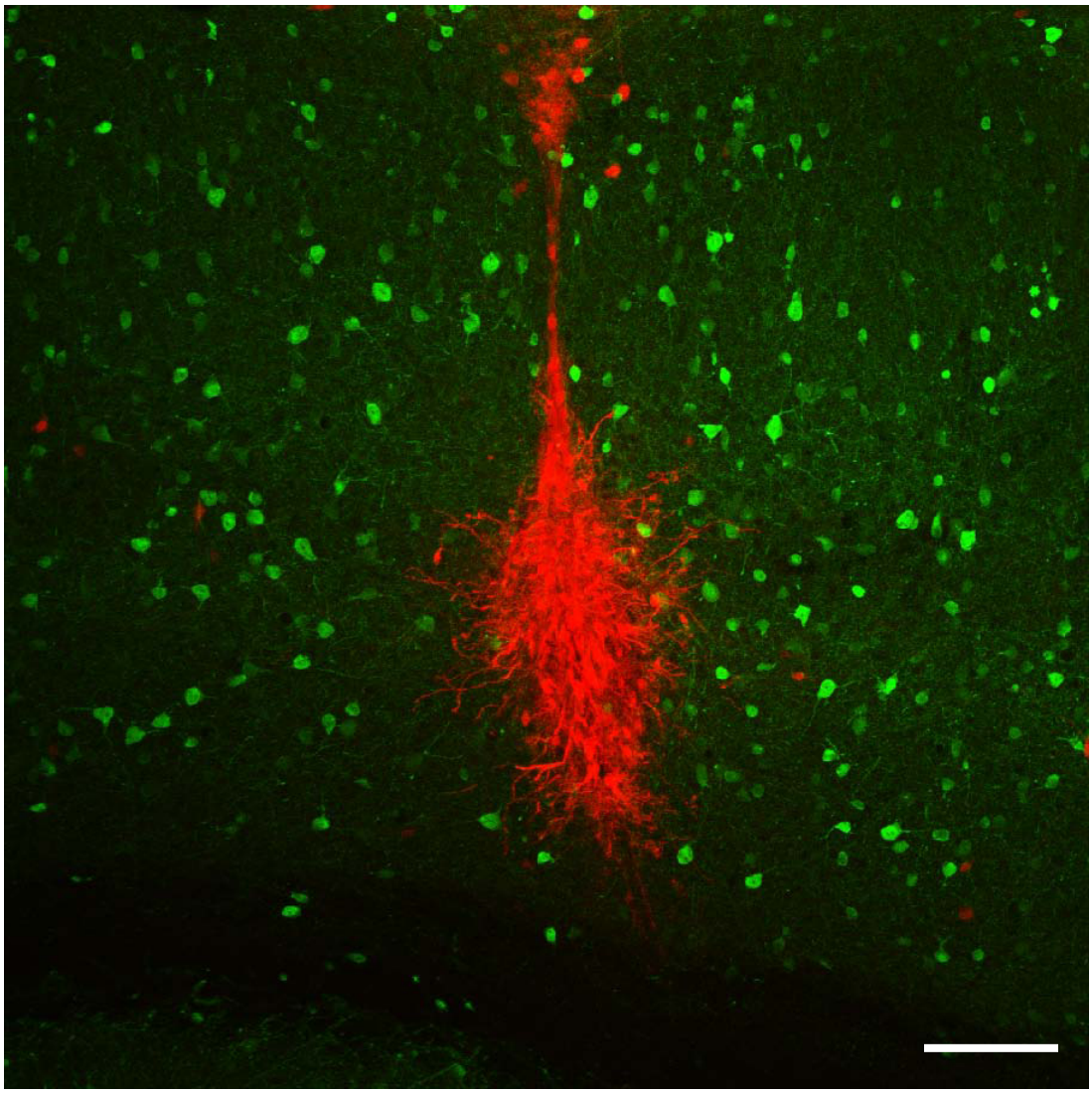

**Figure S3. Transplanted LGE cells remain near the site of transplantation and survive in the host brain.** Host cortex labeled for endogenous GAD67-GFP neurons (green) and transplanted DsRed cells from the E13.5 LGE (red). Animals were assessed for plasticity at 33-35 DAT. Image is oriented with dorsal at top and lateral at left. Scale bar = 100 μm.

# Figures S4-5

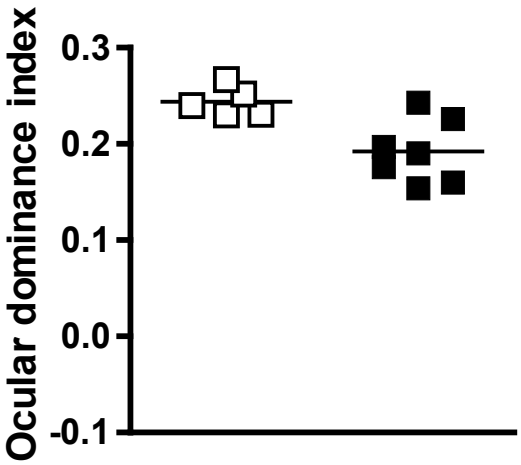


**Figure S4. Transplantation of dead MGE cells does not induce ocular dominance plasticity.** Cells from the MGE were first killed with a cycle of freezing and thawing and then transplanted into P9-11 mice. Hosts were studied for ocular dominance plasticity at P42-45, 33-35 days after transplantation of dead cells. Open squares show visual responses before monocular deprivation (MD) and filled squares show responses after MD. Visual responses were only modestly affected by MD, consistent with the diminution of ocular dominance plasticity seen at these ages after the critical period (*4*).

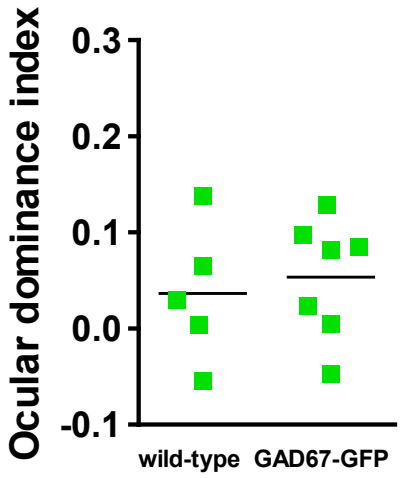


**Figure S5. Similar effects of monocular deprivation (MD) in wild-type and GAD67-GFP recipients 33-35 days after transplantation (DAT).** Four days of MD produced similar effects 33-35 DAT to P9-11 wild-type hosts and P9-11 GAD67-GFP hosts.

# Figure S6

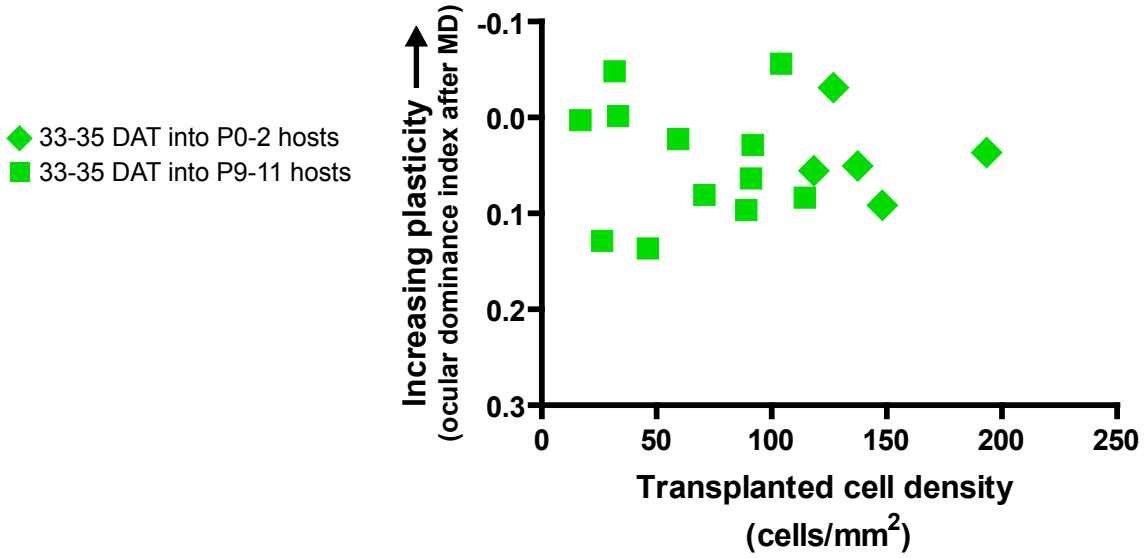


**Figure S6. Transplanted inhibitory neurons induce ocular dominance plasticity 33-35 days after transplantation across a large range of transplanted cell densities.** Plot of ocular dominance index (ODI) after monocular deprivation (MD) versus transplanted cell density for host groups studied at 33-35 DAT. The P9-11 33-35 DAT group includes wild-type (n = 5) and GAD67-GFP (n = 7) host animals. Smaller ODI values represent a stronger effect of MD.

# Figure S7

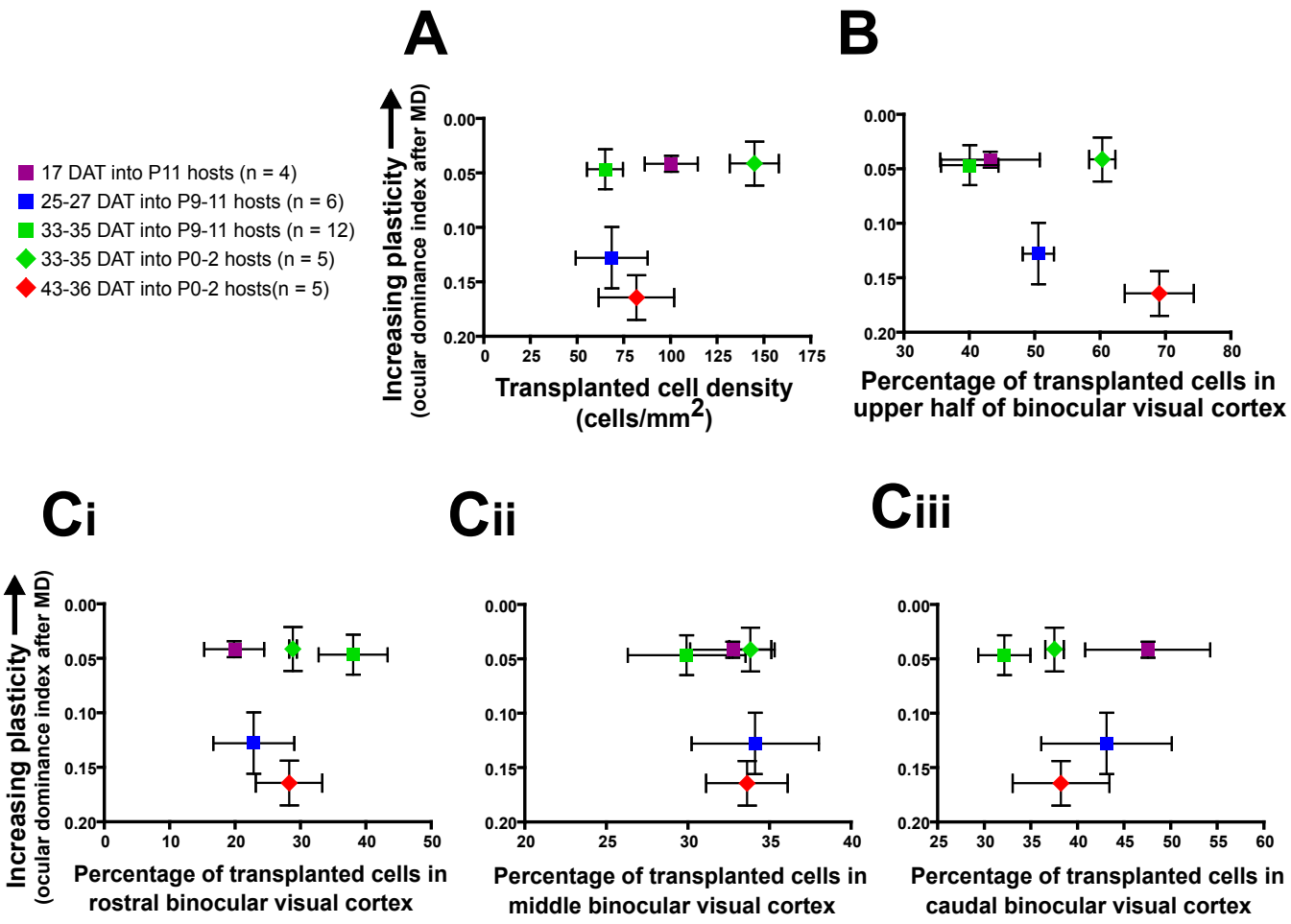


**Figure S7. Variations in transplanted cell densities and spatial distributions do not account for the pronounced plasticity observed 33-35 days after transplantation (DAT).** **(A)** Plot of the mean ocular dominance index (ODI) after monocular deprivation (MD) versus mean transplanted cell densities, shown for groups described in Figure 1. Smaller ODI values represent a stronger effect of MD. The density of cells that produced plasticity at 33-35 DAT (P0-2 host group in green diamonds; P9-11 host group in green squares) were not as effective at producing plasticity at either 25-27 DAT (blue squares) or 43-36 DAT (red diamonds). **(B)** Plot showing ODI after MD versus the percentage of cells in the upper half of host binocular visual cortex. Both lower (40.0%, green squares, P9-11 hosts) and higher percentages (60.3%, green diamonds, P0-2 hosts) of cells in the upper layers were sufficient to induce plasticity 33-35 DAT. **(C i-iii)**. Plots of the percentage of transplanted cells in the rostral **(i)**, middle **(ii)** and caudal **(iii)** parts of host visual cortex versus ODI after MD. The distribution of cells along the rostro-caudal axis also did not account for the selective effect observed at 33-35 DAT. The P9-11 33-35 DAT group includes wild-type (n = 5) and GAD67-GFP (n = 7) hosts. Error bars represent the standard error of the mean.

# Figure S8

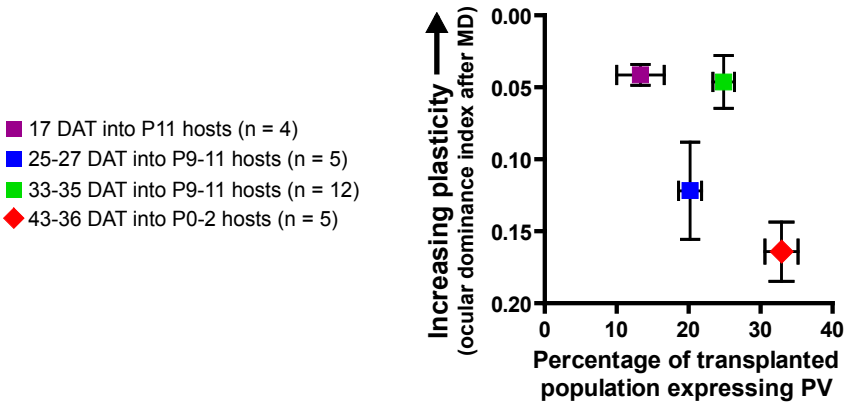


**Figure S8. The abundance of parvalbumin-expressing cells does not account for the pronounced plasticity observed 33-35 days after transplantation (DAT).** Plot of ocular dominance index (ODI) after monocular deprivation (MD) versus the percentage of transplanted cells labeled by parvalbumin (PV), shown for host groups transplanted at P9-11. The P9-11 33-35 DAT group includes wild-type (n = 5) and GAD67-GFP (n = 7) host animals. Smaller ODI values represent a stronger effect of MD. There was no obvious relationship between the extent of ocular dominance plasticity and the percentage of transplanted cells that expressed PV. Error bars represent the standard error of the mean.

# Figure S9

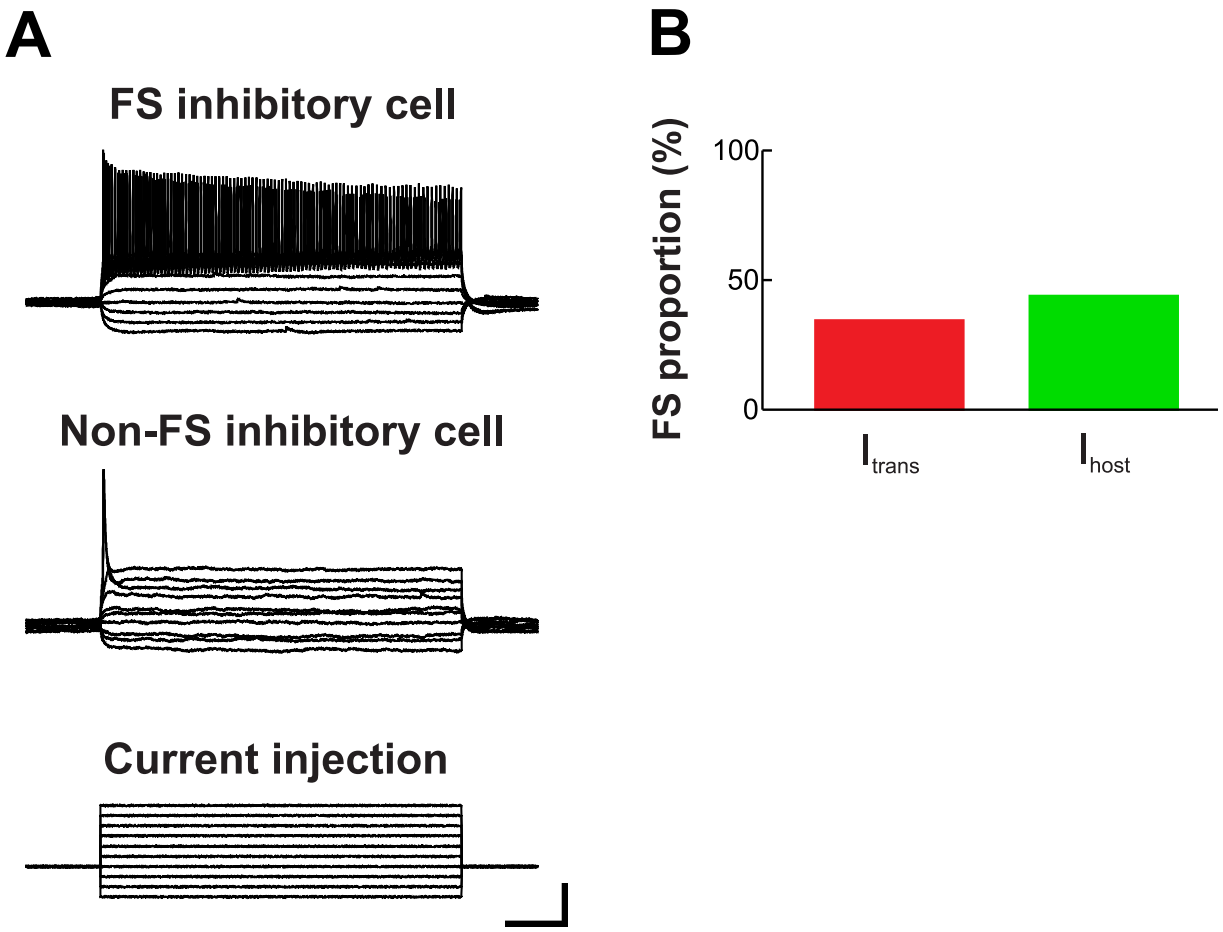


**Figure S9. Transplanted cells exhibit fast-spiking and non-fast-spiking phenotypes, and similar fractions of fast-spiking cells were recorded in the transplanted- and host populations.** (**A**) Representative spiking responses from transplanted inhibitory neurons. Top, fast-spiking (FS) inhibitory neuron; middle, non-FS inhibitory neuron; bottom, current injection used to evoke spikes and measure current-voltage relationships. Scale bar, 100 ms, 20 mV (top and middle); 100 ms, 200 pA (bottom). (**B**) The proportions of transplanted- and host inhibitory neurons that exhibited FS properties were similar. Red, transplanted inhibitory neurons (10/29, 34.5%); green, host inhibitory neurons (11/25, 44.0%; $p > 0.5$, Fisher's two-tailed exact test).

**Notes (Supporting online material)**


S1. A. M. Hadjantonakis et al. Mech. Dev. **76**, 79-90 (1998).

S2. K. Vintersten *et al.* Genesis **40**, 241-246 (2004).

S3. N. Tamamaki, *et al*. J. Comp. Neurol. **467**, 60-79 (2003).

S4. F.T. Merkle, Z. Mirzadeh, A. Alvarez-Buylla, Science **317**, 381-384 (2007).

S5. J. Gordon, M.P. Stryker, J. Neurosci. **16**, 3274-3286 (1996).

S6. M. Kaneko, J. L. Hanover, P. M. England, M. P. Stryker, Nat. Neurosci. **11**, 497-504 (2008).

S7. V. Kalatsky, M. P. Stryker, Neuron **38**, 529-545 (2003).

S8. J. Cang, V. A. Kalatsky, S. Lowel, M. P. Stryker, Vis. Neurosci. **22**, 685-691 (2005).

S9. C.M. Niell, M.P. Stryker, J. Neurosci **28**, 7520-7536 (2008).

S10. S.P. Gandhi, Y. Yanagawa, M.P. Stryker, Proc. Natl. Acad. Sci. U.S.A. **105**, 16797-16802 (2008).

S11. M. Kaneko, D. Stellwagen, R.C. Malenka, M. P. Stryker, Neuron **58**, 673-680 (2008).